

AN ANALYTIC CALCULATION OF THE ELECTRON CLOUD LINEAR MAP COEFFICIENT

U. Iriso[†] and S. Peggs[‡]

[†]CELLS, PO Box 68, 08193 - Bellaterra (Spain)

[‡]BNL, Upton, NY 11973 (USA)

Abstract

The evolution of the electron density during multibunch electron cloud formation can often be reproduced using a bunch-to-bunch iterative map formalism. The coefficients that parameterize the map function are readily obtained by fitting to results from compute-intensive electron cloud simulations. This paper derives an analytic expression for the linear map coefficient that governs weak cloud behaviour from first principles. Good agreement is found when analytical results are compared with linear coefficient values obtained from numerical simulations.

INTRODUCTION

The evolution of the electron cloud from the passage of bunch m to $m+1$ is empirically well represented by a cubic map [1, 2]

$$\rho_{m+1} = a\rho_m + b\rho_m^2 + c\rho_m^3, \quad (1)$$

where ρ [nC/m] is the linear electron density inside the beam pipe. The values for the coefficients a , b , and c are readily obtained by fitting to results from compute-intensive electron cloud simulations. This paper shows an analytical calculation of the linear map coefficient a in Eq. 1 and compares it with those obtained after running CSEC simulations for the Relativistic Heavy Ion Collider (RHIC).

Consider N_m quasi-stationary electrons uniformly distributed in the transverse cross-section of the beam pipe, as shown in Fig. 1. After a bunch passage, we determine the formation of an electron cloud by evaluating these three steps: 1) compute the electron energy gain due to the passage of a bunch with a non-uniform charge distribution [3] 2) compute the number of secondary electrons produced after an electron-wall collision as a function of the electron energy (parameterization of $\delta(E)$ [4]) 3) calculate the electron survival until the next bunch arrives [1]. The survival electrons at step 3) represent N_{m+1} , the number of electrons at bunch passage $m+1$. The coefficient a is $a = N_{m+1}/N_m$ (for small N_m), so that an electron cloud builds up if $a > 1$. A similar calculation was first introduced in Ref. [5], although it did not include the survival time of the electrons.

ENERGY GAIN AND ELECTRON MOTION

A cylindrical beam pipe of radius R_p is considered (RHIC case). In the absence of external electromagnetic

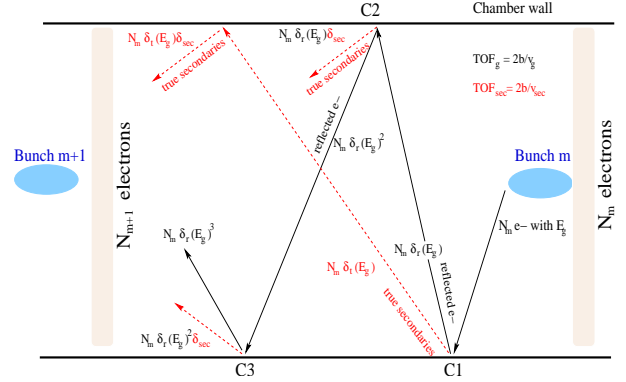


Figure 1: Schematic analysis of the evolution of an electron cloud between two bunch passages. The bunch m accelerates the N_m electrons initially at rest to an energy E_g . The symbol $C1$ marks the first wall collision, when two new “jets” are created: the backscattered one with energy E_g and proportional to δ_r , and the “true secondaries” (with energy $E_{sec} \sim 5eV$ and proportional to δ_t). The sum of all these jets becomes the number of surviving electrons, N_{m+1} .

fields and assuming that the electron motion is limited to the transverse radial direction (transverse plane, electron trajectories crossing along the beam pipe diameter), the time of flight is for an electron with energy E is

$$t_F(E) = \frac{2R_p}{\sqrt{2E/m_e}}, \quad (2)$$

where m_e is the electron mass. The assumption of transverse radial motion implies that the electron-wall collisions are at a perpendicular incidence angle. Although this is not a bad approximation for field free regions, but not valid elsewhere.

Since the “critical radius” is in the same order as the RHIC beam pipe radius R_p , the energy gain is given by [3]

$$E_g = m_e c^2 \frac{N_b r_e}{\sqrt{2\pi\sigma_z}} \left(\ln \frac{R_p}{c_0 \sigma_r} - \frac{1}{2} \right), \quad (3)$$

where N_b is the bunch charge, σ_r and σ_z are the rms bunch radius and length, respectively, $c_0 = 1.05$, r_e is the classical electron radius, m_e is the electron mass, and c is the speed of light.

ELECTRON-WALL COLLISIONS

The Secondary Emission Yield (SEY or $\delta(E)$) gives the number of secondary electrons produced after an electron

of energy E hits a chamber wall. We divide this contribution into “true secondaries” and “reflected” electrons [4, 6]:

$$\delta(E) = \delta_t(E) + \delta_r(E). \quad (4)$$

(See Fig. 2). To avoid long mathematical expressions, we use $\delta_t(E_g) \equiv \delta_t$ and $\delta_r(E_g) \equiv \delta_r$ throughout below. Their distinction is given by the energy at which the secondary electrons are emitted: “true secondaries” are emitted with an energy E_{sec} (typically around 5 eV), while the (elastically) “reflected” electrons are emitted with an energy E_g (see Fig. 3). The contribution of the so-called “rediffused” electrons is neglected in this analysis. Figure 3 shows a comparison between the measured energy distribution curve (red points) and the energy distribution curve assumed in this analysis (blue boxes). The energy distribution curves in this case becomes two Dirac delta functions centered at E_{sec} and E_g (Fig. 3, left), whose height is proportional to δ_t and δ_r , respectively (Fig. 2).

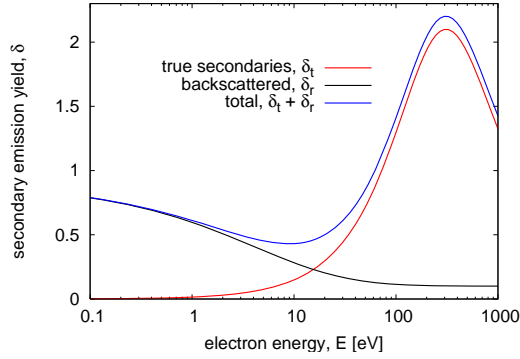


Figure 2: SEY as a function of the electron energy, showing the contribution of the “true secondaries” – δ_t , and the backscattered electrons – δ_r .

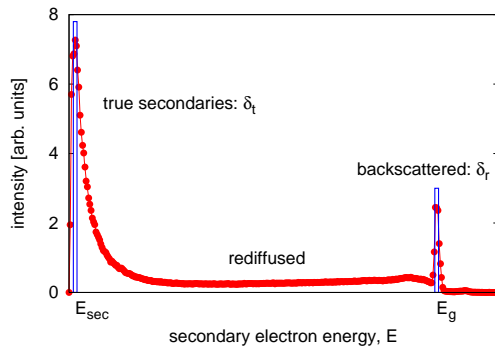


Figure 3: The red points show the measured energy distribution curve in the SEY process, the blue boxes show the energy distribution curve in this analysis: electrons are emitted either with energy E_g (reflected) or E_{sec} (true secondaries). Courtesy of M. Furman [4].

SURVIVING ELECTRONS

Assume now that all the electrons initially at rest gain an energy E_g after the bunch passage. This *monoenergetic* jet collides with the vacuum chamber (marked with $C1$ in Fig. 1). The electrons produced at the chamber wall are [4]

$$N_{C1,\text{sec}} = N_m \delta_t, \text{ true secondaries, and} \quad (5)$$

$$N_{C1,\text{ref}} = N_m \delta_r, \text{ elastically reflected.} \quad (6)$$

The number of elastic collisions the *monoenergetic* jet with energy E_g performs between two bunches is

$$n = \frac{t_{\text{sb}} - t_{\text{FG}}/2}{t_{\text{FG}}}, \quad (7)$$

where t_{sb} is the time between two consecutive bunch passages, and $t_{\text{FG}} \equiv t_F(E_g)$ corresponds to the time of flight of an electron with energy E_g . The high energy electrons before bunch $m+1$ passes by are those provided by the last elastic wall collision at energy E_g . These are [1]:

$$N_{Cn,\text{ref}} = N_m \delta_r^n. \quad (8)$$

For low energy electrons impinging on a surface, there is no fundamental distinction between true secondaries and elastically reflected [6]. All secondary electrons are considered to be produced after elastic processes. Define

$$\delta(E_{\text{sec}}) = \delta_t(E_{\text{sec}}) + \delta_r(E_{\text{sec}}) \equiv \delta_{\text{sec}}, \quad (9)$$

insofar as the secondary electrons are all emitted with the same energy $E_{\text{sec}} \sim 5$ eV. After a Ci collision (see for example collisions $C1$ or $C2$ in Fig. 1), the number of true secondaries is:

$$N_{Gi,\text{ts}} = N_m \delta_r^{i-1} \delta_t \delta_{\text{sec}}^{k_i}, \quad (10)$$

where k_i is the number of collisions for the low energy jet after the Ci^{th} collision:

$$k_i = (n+1-i) \sqrt{E_{\text{sec}}/E_g} \equiv (n+1-i)\xi. \quad (11)$$

The summation of the contribution by all the true secondaries is [1]:

$$\sum_{i=1}^n N_{Ci,\text{sec}} = N_m \delta_t \sum_{i=1}^n \delta_r^{i-1} \delta_{\text{sec}}^{k_i}. \quad (12)$$

THE LINEAR MAP COEFFICIENT

The contributions of both the high and low energy electrons (Eqs. 8 and 12) provides then the total number of electrons at bunch $m+1$, i.e. N_{m+1} . Hence, the linear map coefficient is

$$a = N_{m+1}/N_m = \delta_r^n + \delta_t \delta_{\text{sec}}^\xi \frac{\delta_{\text{sec}}^\xi - \delta_r^n}{\delta_{\text{sec}}^\xi - \delta_r}. \quad (13)$$

Recall that the terms in δ_t , δ_r , n , and ξ are functions of the energy gain produced by the bunch passage (parameter E_g , see Eq. 3), while n is also a function of the bunch

spacing as well. Thus, Eq. 13 merges beam and wall surface chamber parameters in a single expression and eases parameter space analysis. Note for example, that $a \rightarrow 0$ as $n \rightarrow \infty$ (infinitely long bunch spacing). However, if $\delta_0 \rightarrow 1$, $a \rightarrow \delta_t/(1-\delta_r)$, which shows that electron clouds can occur even for an infinitely long bunch spacing!

This calculation of a has been performed assuming only one *monoenergetic* jet of energy E_g results from the electron-bunch interaction. More realistic calculations should involve not a single jet with energy E_g but the distribution of the energy spectrum $h(E)$:

$$a = \int_0^\infty \left[\delta_r(E)^{n(E)} + \delta_t(E) \delta_{\text{sec}}^{\xi(E)} \frac{\delta_{\text{sec}}^{n(E)} \xi(E) - \delta_r^{n(E)}}{\delta_{\text{sec}}^{\xi(E)} - \delta_r(E)} \right] h(E) dE \quad (14)$$

From this expression, it is compelling to call the parameter a the **effective secondary emission yield** of the beam pipe wall, δ_{eff} , depending on both the chamber material and the beam characteristics. This analysis allows to easily study thresholds beyond which electron cloud formation occurs. Figure 4 shows two examples of how a evolves as a function of the bunch spacing for the beam and chamber parameters listed in Table 1.

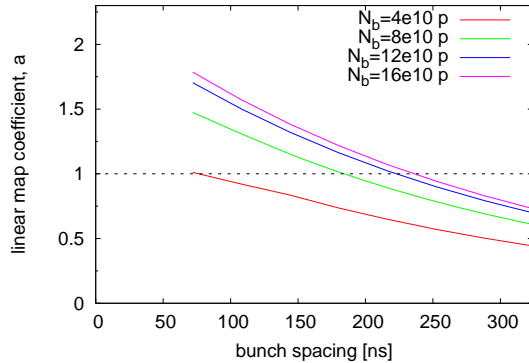


Figure 4: Analytical prediction of a as a function of the bunch spacing.

COMPARISON WITH SIMULATION FITS

Figure 5 compares the results of calculations of the linear map coefficient a using this analytical method (lines) and after fitting the CSEC simulation results (marks) as a function of the bunch population and for different δ_{max} . The color of the marks and lines coincide for the same δ_{max} . Both results agree acceptably in the general evolution of the parameter a . We stress that the largest disagreement occurs when $N > 12 \times 10^{10}$ protons/bunch. This is arguably related to the neglect of the rediffused electrons, which might play an important role when the energy gain E_g due to the bunch passage is larger than the energy at which the SEY has its maximum, E_{max} .

Table 1: Beam and SEY parameters used for the calculations in Figs. 4 and 5.

parameter	value
beam pipe radius, b [cm]	6
bunch spacing, t_{sb} [ns]	107
maximum SEY, δ_{max}^*	1.9
SEY for $E \rightarrow 0$, δ_0	0.7
rms bunch length, σ_z [m]	1
true second. energy, E_{sec} [eV]	5
SEY at $E \rightarrow \infty$, δ_∞	0.15
energy for max. δ , E_{max} [eV]	300
rms beam size, σ_r [mm]	2

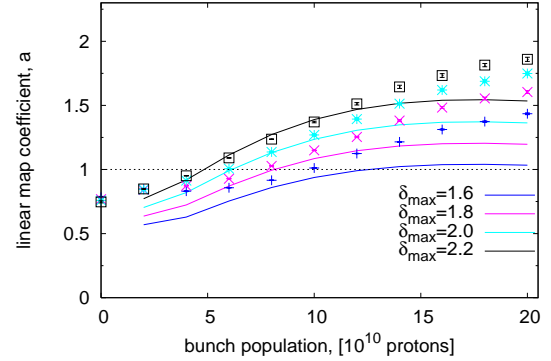


Figure 5: Comparison of the linear map coefficient a derived using CSEC simulations (symbols) and using the analysis in this report (lines with the same color), as a function of the bunch population N for different values of δ_{max} .

SUMMARY

The linear map coefficient a is derived from first principles. The expression merges both beam and vacuum chamber characteristics, and it is in an acceptably good agreement when compared with results obtained after CSEC simulations. The analysis is useful to determine safe regions in parameter space where an accelerator can be operated without creating electron clouds. The formalism shows that electron clouds can occur for long bunch spacings if $\delta_0 \rightarrow 1$.

REFERENCES

- [1] U. Iriso. *Electron Clouds in the Relativistic Heavy Ion Collider*. PhD Thesis, Univ. of Barcelona, January 2006. BNL internal report C-A/AP/228.
- [2] U. Iriso and S. Peggs. *Maps for Electron Clouds*. PRST-AB 8, 024403, Jan. 2005.
- [3] S. Berg. *Energy gain in an electron cloud during the passage of a bunch*. CERN, LHC Project Report 97, 1997.
- [4] M. Furman and M. Pivi. *Microscopic probabilistic model for the simulation of secondary electron emission*. PRST-AB 5, 12404, 2002.
- [5] G. Stupakov. *Photoelectrons and Multipacting in the LHC: Electron Cloud Build-up*. CERN, LHC Project Report 141, 1997.
- [6] R. Cimino, I. Collins, M. Furman, M. Pivi, G. Rumolo, F. Zimmermann. Phys. Rev. Lett. **93**, 014801 (2004).